Jurnal Kejuruteraan 38(5) 2026: 2617-2624
https://doi.org/10.17576/jkukm-2026-38(5)-39

Enhancing Antibacterial Properties Using Silver Doped Zinc Oxide Nanoparticles

Nur Farihah Alya Adanan, Affa Rozana Abdul Rashid* & Mohd Riza Mohd Roslan

Faculty of Science and Technology, Universiti Sains Islam Malaysia (USIM) Bandar Baru Nilai, 71800 Nilai, Negeri Sembilan

**Corresponding author: affarozana@usim.edu.my*

Received 2 January 2026, Received in revised form 29 April 2026
Accepted 29 May 2026, Available online 30 August 2026

ABSTRACT

This study investigates the enhancement of material properties with a particular focus on the antibacterial performance of Ag-doped ZnO for potential biomedical applications. Undoped ZnO often exhibits limited antibacterial efficiency, therefore, this study investigates property enhancement through controlled Ag doping. Undoped and Ag-doped ZnO nanoparticles were synthesized via the precipitation method using silver (Ag) doping concentrations of 0.2%, 0.6%, and 1.0%. X-ray diffraction (XRD) revealed that the crystallite size decreased from 42.97 nm for undoped ZnO to to 43.18 nm, 36.39 nm, and 36.26 nm for 0.2%, 0.6%, and 1.0% Ag-doped ZnO, respectively, indicating inhibited crystal growth with increasing Ag content. Fourier-transform infrared spectroscopy (FTIR) confirmed the Zn–O and Ag–O stretching vibrations at 500–600 cm^{-1}, verifying the successful synthesis. Field emission scanning electron microscopy (FESEM) showed agglomerated plate-like structures in undoped ZnO, while Ag-doped samples exhibited smaller, compact, and densely clustered morphologies, demonstrating the influence of Ag incorporation on surface features. Energy-dispersive X-ray (EDX) analysis confirmed Zn and O as main constituents, with Ag signals detected up to 1.51 weight % in the 1%Ag-doped sample, validating successful doping. Antibacterial activity, tested using the disc diffusion method against Escherichia coli, showed an average inhibition zone of 15.67 mm for undoped ZnO, increasing to 19.33 mm at 0.2%Ag-doped ZnO, highlighting enhanced antibacterial performance. These findings provide valuable insights into the potential of Ag-doped ZnO as an advanced material for biomedical and health-related applications.

Keywords: Antibacterial coatings; Ag-doped ZnO; Precipitation method; disc diffusion method; Escherichia coli (E. coli)

INTRODUCTION

Orthopaedic implant surgeries, which are crucial in restoring mobility and improving quality of life, carry a particularly high risk of implant-associated infections (IAIs). This is primarily due to the invasive nature of surgery and the presence of indwelling devices within the patient's body. Usually, post-surgical infections commonly caused by *Staphylococcus aureus* (S. Aureus), which may result in chronic infection, implant loosening, and the need for costly secondary surgeries, thereby imposing significant financial and emotional burdens on patients and healthcare systems (Weber et al. 2018). The primary cause of IAIs is bacterial biofilm formation on implant surfaces (Li et al. 2023), where bacteria develop a protective matrix that reduces antibiotic effectiveness and host immune response. Hence, this condition can subsequently contribute to the development of antimicrobial resistance (AMR). Based on Khatoon et al. (2018), current treatment strategies, such as systemic antibiotics, face growing challenges due to the antibiotic resistance and the bacteria biofilm formation. World Health Organization (WHO) has also identified that AMR as one of the top global health threats, with hospital-acquired infections contributing significantly to patient's sickness and death (Abdelazeem Algammal et al. 2023; Monegro et al. 2023).

Given the growing concern of implant-associated infections (IAIs) and antimicrobial resistance (AMR), there is an urgent need for improved surface modification strategies for orthopaedic implants. The existing solutions such as coating technologies based on hydroxyapatite (HAP) and titanium have shown promising potential, however, they are limited by high cost, instability, or poor compatibility with the mechanical properties of bone (Accioni et al. 2022; Amirtharaj Mosas et al. 2022). In Malaysia, stainless steel implants are widely used in government hospitals due to their affordability and mechanical strength. However, these implants are generally limited to electropolishing surface treatments, which lack antibacterial functionality (Han & Fang 2019). This highlights the need for cost-effective antibacterial coatings specifically tailored for stainless steel implants.

Hence, zinc oxide (ZnO) has emerged as a promising candidate due to its abundance, low cost, biocompatibility, and natural antibacterial activity through reactive oxygen species (ROS) generation (Carofiglio et al. 2020; Abinaya et al. 2016). However, the antibacterial performance of ZnO alone remains limited and can be further enhanced through doping with various dopants. Among the noble metal elements, silver (Ag) is particularly effective, as it provides synergistic antimicrobial effects and extends ZnO's photocatalytic activity into the visible light region (Vaishali Amrute et al. 2024). As a result, it will enhance the material's efficiency in pollutant degradation. Puspasari et al. (2022) also reported that the combination of Ag and ZnO produces a composite material with superior antibacterial activity compared to either component alone. Furthermore, ZnO has been extensively explored as a functional material for a wide range of sensing applications, including ultraviolet (UV) detection, alcohol sensing, uric acid detection, and related analytes (Rashid et al. 2019; Rashid et al. 2024).

The antibacterial efficacy of Ag-doped ZnO strongly dependent on dopant concentration, with 0.2–1.0% Ag commonly reported as the optimal range for balancing antibacterial performance and biocompatibility (Geioushy et al. 2024). However, concerns have been raised regarding the cytotoxicity effects of Ag at higher concentrations (Bondarenko et al. 2013) Therefore, lower Ag concentration are generally preferred to minimize potential cytotoxicity. Therefore, lower Ag concentrations are generally preferred to minimize potential cytotoxicity. Geioushy et al. (2024) further reported that 1.0% Ag often yields the strongest and most sustained antibacterial performance. Based on these considerations, this study selected 1.0% as the maximum and 0.2% as the minimum Ag doping concentrations.

Nevertheless, several gaps remain in identifying the optimal doping concentration that yields maximum antibacterial efficiency while maintaining a cost-effective synthesis approach. Furthermore, limited research has investigated ZnO and Ag doped ZnO as coatings for stainless steel orthopaedic implants. Moreover, few studies have systematically compared undoped ZnO with Ag-ZnO across a range of concentrations against both Gram-positive and Gram-negative bacteria. To address these gaps, this study synthesizes undoped and Ag doped ZnO nanoparticles via the precipitation method and evaluates their structural, morphological, and antibacterial properties.

METHODOLOGY

PREPARATION OF AG DOPED ZNO

Undoped ZnO was synthesized using the precipitation method. An aqueous solution of 0.3 M was prepared by dissolving 11 g of zinc acetate dihydrate $(Zn(CH_3COO)_2 \cdot 2H_2O$ in 200 ml of distilled water. The solution was stirred continuously for 15 minutes at room temperature to obtain a homogenous mixture. In a separate beaker, 6 g of sodium hydroxide pellet (NaOH, 98%, M.W. 40) were dissolved in 200 ml of distilled water. The NaOH solution was then added dropwise into the $Zn(CH_3COO)_2 \cdot 2H_2O$ solution. The reaction mixture was stirred at room temperature for 2 hours, resulting in the formation of a white precipitate. The suspension was subsequently aged for an additional 2 hours at room temperature. The precipitate was collected by vacuum filtration and washed several times with distilled water to remove residual impurities. The obtained product was then oven-dried at 60 °C for 4 hours. Finally, the dried sample was annealed at 500 °C for 2 hours to obtain ZnO nanoparticles. For Ag doped ZnO, the synthesis procedure was identical to the preparation of undoped ZnO, except silver nitrate ($AgNO_3$, M.W. 169.87, Scharlau Chemicals) was introduced as the dopant precursor. Specifically, 0.017 g, 0.0511 g, and 0.0851 g of $AgNO_3$ were prepared to obtain Ag doping concentrations of 0.2%, 0.6%, and 1.0%, respectively. The $AgNO_3$ was subsequently added to zinc acetate solution under continuous stirring. The subsequent mixing and processing steps were carried out following the same procedure as described for the undoped ZnO synthesis.

MATERIAL CHARACTERIZATION

The synthesized samples were characterized using various analytical techniques to investigate their morphological, structural and chemical properties. The crystalline structure was examined by X-ray diffraction (XRD) employing Cu Kα radiation (λ = 1.5406 Å) at an operating voltage of 40 kV and a current of 30 mA. The X-ray diffraction measurements were performed over a scanning range of

$2\theta = 10°–80°$, with a step width of 0.02°. The obtained data were used to identify the crystalline phases, and the average crystallite size was estimated using the Scherrer equation. The Scherrer's (equation 1) was used to calculate the crystallite sizes.

$$D = \frac{k\lambda}{\beta \cos\theta} \quad (1)$$

where D represents the crystallite size, λ denotes the wavelength of the Cu Kα radiation (1.5406 Å), k is the shape factor (0.9), β corresponds to the full width at half maximum (FWHM) of the selected diffraction peak, and θ is the Bragg angle. The crystallite size was calculated using the most intense diffraction peaks. The surface morphology and particle distribution were examined using Field Emission Scanning Electron Microscopy (FESEM) (JEOL JSM-7001F), which provided high-resolution images of the material structures. Energy Dispersive X-ray (EDX) was used to determine the material composition and confirming the presence of zinc, oxygen, and silver elements in the samples. The chemical bonding and functional groups present were identified by Fourier Transform Infrared (FTIR) spectroscopy (Thermo Scientific Nicolet iS50) in the wavenumber range of 4000–400 cm^{-1}. The spectra revealed characteristic absorption bands corresponding to metal–oxygen stretching and hydroxyl group vibrations.

ANTIBACTERIA TEST

SAMPLE AND CULTURE MEDIA PREPARATION

Sample preparation, including the preparation of positive and negative controls was carried out prior to microbial testing. The synthesized powders were compressed into uniform discs (≈0.5 g each) using a hydraulic press. For control preparation, 6 mm paper discs were infused with 10 µL of distilled water to serve as negative controls, while discs containing 10 µg of streptomycin were used as the positive control.

Subsequently, Mueller-Hinton (MH) agar plates were prepared. Mueller-Hinton agar (MHA) was prepared by dissolving 6.8 g of MHA powder in 200 mL of distilled water. Then followed by sterilization in an autoclave at 121˚C for 15 minutes. Under sterile condition in a laminar flow hood, approximately 25 mL of solution was poured into each Petri dish to achieve an agar depth of about 4 mm. Next, allowed sufficient time for complete desiccation. Each MHA plate was then divided into 4 quadrants to accommodate multiple discs. In this study, every sample requires 6 quadrants to place the triplicate of undoped ZnO or Ag-ZnO samples, along with paper disc infused with distilled water, streptomycin as positive control, and Phosphate-buffered saline (PBS) as negative control enabling direct comparison of inhibition zones under identical conditions.

DISC DIFFUSION METHOD

The antibacterial activity of the synthesized samples was evaluated using the disc diffusion method against *Escherichia coli*. Phosphate-buffered saline (PBS) was prepared by dissolving one PBS tablet in 500 mL of distilled water, followed by sterilized at 121 °C for 15 minutes. A bacterial inoculum was obtained by transferring *E. coli* culture into a sterile microcentrifuge tube containing 3 mL of PBS. The optical density (OD) of the suspension was measured at 600 nm using a UV–visible spectrophotometer. The bacterial concentration was subsequently adjusted by adding either PBS or bacteria culture to achieve an OD value in the range of 0.1 until 0.2, corresponding to the 0.5 McFarland standard.

Furthermore, serial dilution was performed using sterile saline solution on the bacterial culture (Rashid et al., 2020). A 1 mL of bacterial culture was transferred into a test tube containing 9 mL of PBS to achieve a 10-fold dilution (10^{-2}). After serial dilution, the diluted culture was evenly streaked back and forth over the entire surface of MHA using a sterile cotton swab to create a bacteria lawn and the plate was allowed to dry. The plates were then incubated at 37 °C for 18 hours. After incubation, the zones of inhibition (ZOI) were measured to evaluate the antibacterial activity of the samples. All procedures were carried out in accordance with Clinical and Laboratory Standards Institute (CLSI) guidelines.

RESULTS AND DISCUSSIONS

MORPHOLOGY AND STRUCTURAL PROPERTIES OF AG DOPED ZNO

Distinct changes in the surface morphology of ZnO nanoparticles were observed upon the incorporation of Ag dopants. Undoped ZnO showed irregular and agglomerated particles as shown in Figure 1(a), a typical characteristic due to high surface energy. With 0.2% Ag incorporation in Figure 1(b), the particles became finer and more uniformly dispersed, indicating that silver reduced clustering and improved surface separation. At 0.6% Ag doping (Figure 1(c)), the nanoparticles appeared smaller and more homogeneous with well-defined boundaries, suggesting that Ag effectively regulated nucleation and growth. However, further increase to 1.0% Ag (Figure 1(d)) resulted in slight coarsening and renewed agglomeration, implying that excessive Ag disrupted structural uniformity. These observations aligned with Kusdianto et al. (2025), who reported that Ag addition enhances dispersion and surface uniformity in ZnO nanostructures.

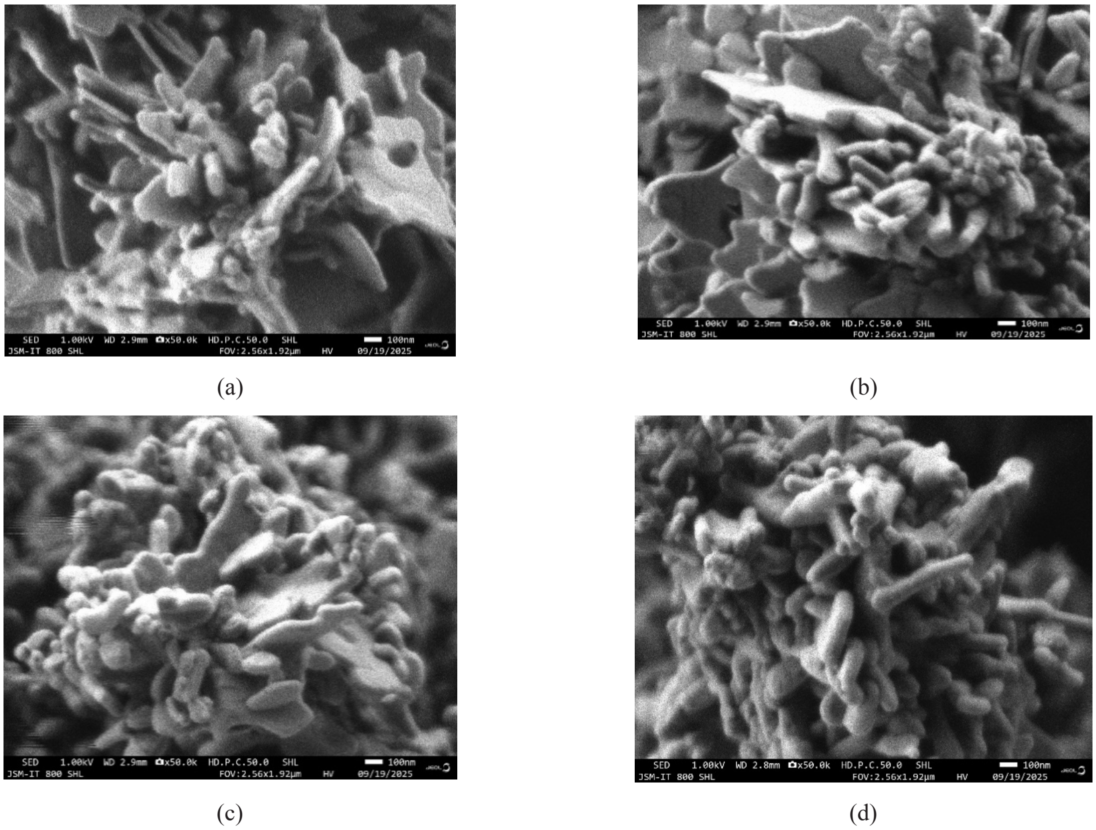

FIGURE 1. Surface morphology of (a) undoped ZnO, (b) 0.2%, (c) 0.4% and (d) 0.6% of Ag doped ZnO

Energy-dispersive X-ray (EDX) analysis confirmed the presence of Zn, oxygen (O), and Ag elements, indicating the successful incorporation of Ag into the ZnO matrix as shown in Table 1. Undoped ZnO displayed only Zn, O, sodium (Na), and carbon (C) signals, while Ag peaks appeared in doped samples and increased proportionally with the doping level. The Ag content increased from 0.14 wt% at low doping to 1.51 wt% at higher doping, demonstrating effective incorporation of silver within the ZnO structure. Minor traces of C and Na were attributed to surface contamination during sample preparation. It could be because the usage of zinc acetate dihydrate ($Zn(CH_3COO)_2 \cdot 2H_2O$) and sodium hydroxide (NaOH) in the precipitation method.

TABLE 1. Materials Composition in EDX

Sample	Zn (wt%)	O (wt%)	Ag (wt%)
A (Undoped ZnO)	48.42	17.82	–
B (0.2% Ag-ZnO)	45.42	17.09	0.14
C (0.6% Ag-ZnO)	66.62	16.81	0.35
D (1.0% Ag-ZnO)	67.48	15.69	1.51

Additionally, XRD analysis proved that all synthesized samples maintained a hexagonal wurtzite ZnO structure with strong and sharp diffraction peaks, indicate good crystallinity as shown in figure 2. The undoped ZnO exhibited major peaks at 2θ values of 31.876°, 34.539°, 36.364°, 47.648°, 56.686°, 62.950°, 66.458°, 68.035°, 69.175°, 72.661°, and 77.033°, corresponding to the (100), (002), (101), (102), (110), (103), (200), (112), (201), (004), and (202) reflection planes, respectively, align with the standard JCPDS card no. 79–0208 for hexagonal ZnO

(Kareem et al. 2022). Upon Ag doping, additional low-intensity peaks appeared at approximately 38.14°–38.20°, which correspond to the (111) reflection plane of metallic silver (Kareem et al. 2022), Proving that Ag was substituted into the ZnO crystal.

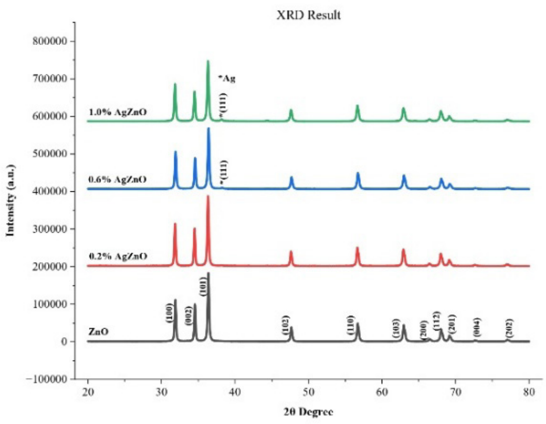

FIGURE 2. XRD patterns of samples

Using the Scherrer's equation, the average crystallite size of the undoped ZnO was 42.97 nm, which slightly increased to 43.18 nm at 0.2% Ag doping. This minor increase can be attributed to the replacement of Zn^{2+} ions which has ionic radius 0.074 nm by larger Ag^{+} ions which the ionic radius is 0.126 nm, led to a small structural expansion (Vaishali Amrute et al. 2024). However, further increase in Ag concentration to 0.6% and 1.0% resulted in a significant reduction of crystallite size to 36.39 nm and 36.26 nm, respectively. This decrease suggests that adding excess silver can cause strain and defects in the ZnO structure, which delay the normal growth of the crystals. This trend matches well with the observations reported by Vaishali Amrute et al. (2024), where low levels of Ag doping initially enhanced crystal size, while higher concentrations caused a reduction due to induced lattice stress. The decrease in crystallite size at higher Ag content suggests an increase in surface area, which could potentially enhance surface-related properties such as photocatalytic efficiency and antimicrobial activity.

FTIR spectra in figure 3 show a strong absorption band within 500–600 cm^{-1}, attributed to Zn–O stretching vibrations, confirming ZnO formation (Vaishali Amrute et al. 2024). In the Ag-doped samples, this band exhibited a slight shift and an additional Ag–O stretching feature, indicating successful Ag incorporation. Absorption bands around 1500–1700 cm^{-1} assigned to C=O stretching from residual organic compounds, while weak peaks between 2000–2200 cm^{-1} associated with atmospheric CO_2 adsorption. The increased intensity of Zn–O vibrations in doped samples reflects the enhancement of lattice interactions due to Ag substitution. It was consistent with the observed decrease in crystallite size from XRD analysis.

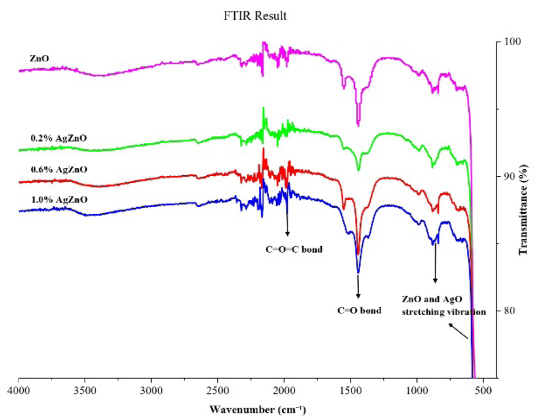

FIGURE 3. FTIR spectra of samples

ANTIBACTERIAL ACTIVITY

After an incubation period of 18 hours at 37 °C, distinct zones of inhibition (ZOI) were observed around the streptomycin disc in quadrant 1, confirming its effectiveness as a positive control. The ZOI value of streptomycin ranged from 16 to 22 mm, specifically 21 mm (Figure 4(a)), 20 mm (Figure 4.b), 16 mm (Figure 4(c)) and 22 mm (Figure 4(d)). In contrast, both phosphate-buffered saline (PBS) and distilled water, used as negative controls in quadrants 3 and 4, showed no visible ZOI, indicating the absence of inherent antibacterial activity. As summarized in Table 2, it is the average ZOI values measured for the tested samples.

From the result of disc diffusion test, a clear relationship between the structural characteristics of the nanoparticles and their antimicrobial performance can be seen. The result showed that the more silver added to the ZnO, the smaller the particle size. It is as mentioned by Mahesh Kumar Talari et al. (2012) how the presence of silver is related to the decrease in crystallite size and can contribute to the enhancement of antimicrobial activity. Similarly, Yamamoto, as cited by Mahesh Kumar Talari et al. (2012), found that smaller ZnO particle sizes increased antibacterial effectiveness against *E. coli* and *S. aureus*, showed that finer particles promote stronger microbial inhibition. However, in this project, it was identified that the 0.2% Ag-doped ZnO sample or in the EDX analysis, only 0.14% of Ag was successfully doped in the ZnO, have the largest zone of inhibition (ZOI). This implies that even a minimal presence of silver can effectively improve the antimicrobial activity of ZnO nanoparticles.

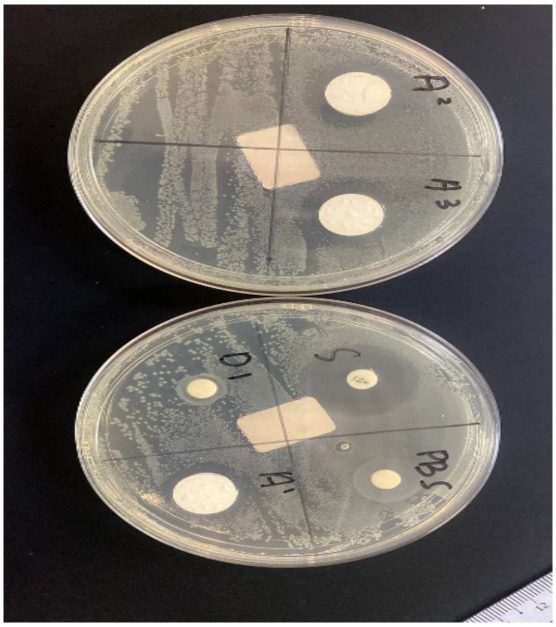

(a)

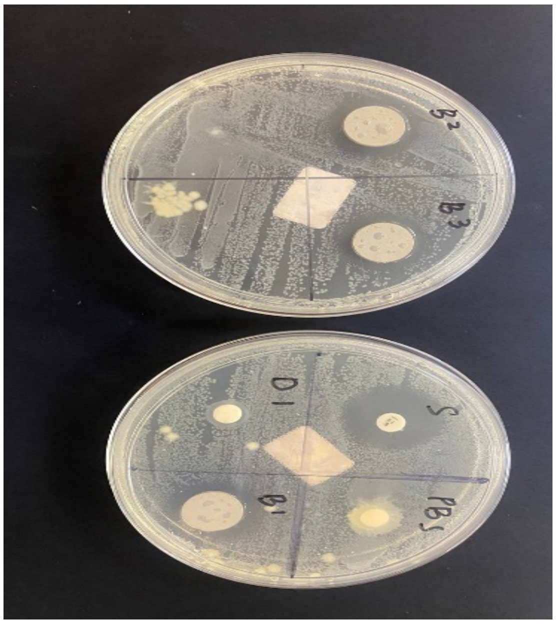

(b)

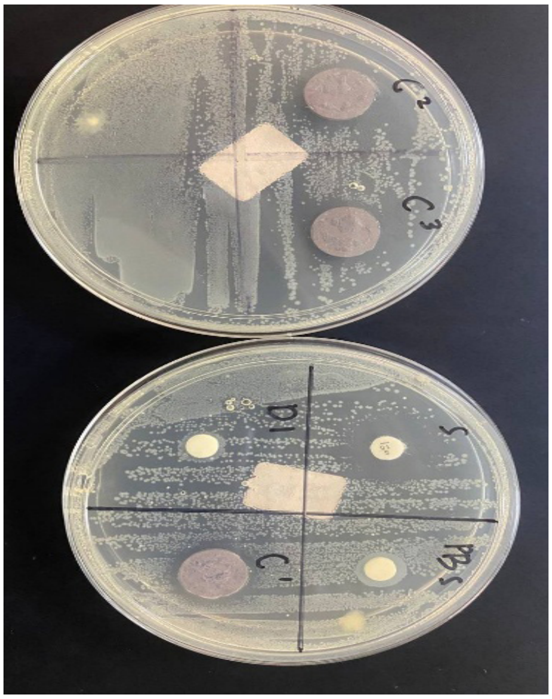

(c)

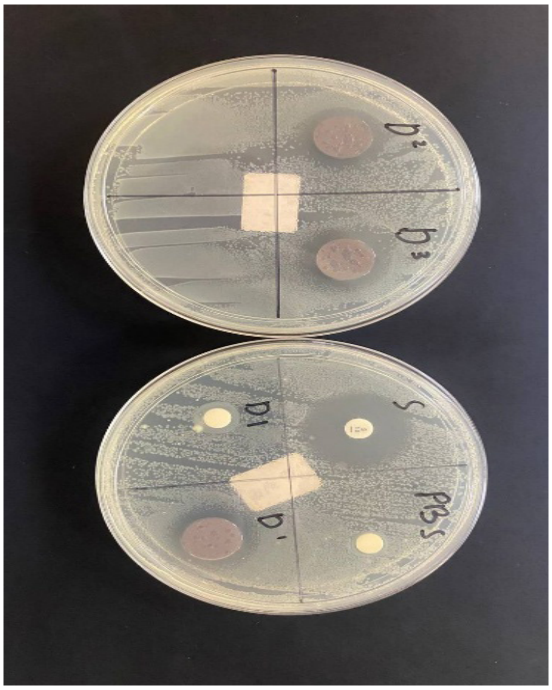

(d)

FIGURE 4. Result of disc diffusion test after 18 hours (a) undoped, (b) 0.2%, (c) 0.4% and (d) 0.6% of Ag-ZnO

TABLE 2. Zone of Inhibition for each sample

Sample	Description	Average ZOI (mm)
A	Undoped ZnO	15.67
B	0.2%Ag-ZnO	19.33
C	0.6% Ag-ZnO	16.67
D	1.0% Ag-ZnO	18.33

The strong antibacterial effect of Ag-doped ZnO in this study can be linked to several complementary mechanisms. The introduction of silver into the ZnO structure improves its bacterial-killing ability through ion release and oxidative reactions. ZnO can create Reactive Oxygen Species (ROS), such as hydrogen peroxide, which damage key cell components like proteins, lipids, and DNA (Mahesh Kumar Talari et al. 2012). This will eventually lead to cell death. Vaishali Amrute et al. (2024) also noted that Ag-doped ZnO generates additional reactive species, including superoxide and hydroxyl radicals, creating oxidative stress that weakens bacterial cells. Hence, these reactive species attack vital components within bacterial cells, including proteins, lipids, and DNA, leading to oxidative stress and ultimately cell death.

CONCLUSION

In summary, this study successfully synthesized and characterized Ag doped ZnO nanoparticles using a simple precipitation method which technically an affordable method. The result demonstrated the enhancement of antibacterial activity against E. coli, with 0.2% of Ag dopant showing the most effective inhibition zone of 19.33 mm. The incorporation of silver effectively suppressed ZnO crystal growth and produced smaller, denser nanoparticles, confirming improved structural and functional properties.

The findings also highlight the importance of controlled synthesis conditions, where careful optimization of parameters such as silver doping concentration, temperature, pH, and mixing conditions plays a crucial role in achieving consistent nanoparticle formation and enhanced antibacterial performance. The study emphasizes that the effectiveness of Ag incorporation is not solely dependent on concentration, but on achieving an optimal balance that maximizes antibacterial efficiency. The absence of cytotoxicity evaluation restricts assessment of the material's biocompatibility and potential toxicity in biomedical applications. Overall, this work demonstrates the strong potential of Ag-doped ZnO nanoparticles as an effective and scalable antibacterial material. With its low-cost synthesis approach and improved functional performance, this material shows promising prospects for future development in biomedical and antimicrobial applications, particularly in areas requiring efficient and reliable antibacterial coatings.

ACKNOWLEDGEMENT

This project acknowledges the facilities and staff assistance Faculty of Science and Technology, Universiti Sains Islam Malaysia (USIM).

DECLARATION OF COMPETING INTEREST

The authors would like to thank Universiti Sains Islam Malaysia (USIM) for the resources and through grant scheme PPPI/USIM/FST/USIM/110823 provided.

REFERENCES

Algammal, A., Hetta, H. F., Mabrok, M. & Behzadi, P. 2023. Editorial: Emerging multidrug-resistant bacterial pathogens "superbugs": A rising public health threat. *Frontiers in Microbiology* 14. https://doi.org/10.3389/fmicb.2023.1135614

Accioni, F., Vázquez, J., Merinero, M., Begines, B. & Alcudia, A. 2022. Latest trends in surface modification for dental implantology: Innovative developments and analytical applications. *Pharmaceutics* 14(2): 455. https://doi.org/10.3390/pharmaceutics14020455

Amirtharaj Mosas, K. K., Chandrasekar, A. R., Dasan, A., Pakseresht, A. & Galusek, D. 2022. Recent advancements in materials and coatings for biomedical implants. *Gels* 8(5): 323. https://doi.org/10.3390/gels8050323

Bondarenko, O., Juganson, K., Ivask, A., Kasemets, K., Mortimer, M. & Kahru, A. 2013. Toxicity of Ag, CuO and ZnO nanoparticles to selected environmentally relevant test organisms and mammalian cells in vitro: A critical review. *Archives of Toxicology* 87(7): 1181–1200. https://doi.org/10.1007/s00204-013-1079-4

Abinaya, C., Marikkannan, M., Manikandan, M., Mayandi, J., Suresh, P., Shanmugaiah, V., Ekstrum, C. & Pearce, J. M. 2016. Structural and optical characterization and efficacy of hydrothermal synthesized Cu and Ag doped zinc oxide nanoplate bactericides. *Materials Chemistry and Physics* 184: 172–182. https://doi.org/10.1016/j.matchemphys.2016.09.039

Carofiglio, M ., B arui, S ., C auda, V. & L aurenti, M. 2020a. Doped zinc oxide nanoparticles: Synthesis, characterization and potential use in nanomedicine. *Applied Sciences* 10(15): 5194. https://doi.org/10.3390/app10155194

Carofiglio, M ., B arui, S ., C auda, V. & L aurenti, M. 2020b. Doped zinc oxide nanoparticles: Synthesis, characterization and potential use in nanomedicine. *Applied Sciences* 10(15): 5194. https://doi.org/10.3390/app10155194

Geioushy, R. A., El-Sherbiny, S., Mohamed, E. T., Fouad, O. A. & Samir, M. 2024. Mechanical characteristics and antibacterial activity against *Staphylococcus aureus* of sustainable cellulosic paper coated with Ag and Cu modified ZnO nanoparticles. *Scientific Reports* 14(1). https://doi.org/10.1038/s41598-024-79265-7

Han, W. & Fang, F. 2019. Fundamental aspects and recent developments in electropolishing. *International Journal of Machine Tools and Manufacture* 139: 1–23. https://doi.org/10.1016/j.ijmachtools.2019.01.001

Kareem, M. A., Bello, I. T., Shittu, H. A., Sivaprakash, P., Adedokun, O. & Arumugam, S. 2022. Synthesis, characterization, and photocatalytic application of silver doped zinc oxide nanoparticles. *Cleaner Materials* 3: 100041. https://doi.org/10.1016/j.clema.2022.100041

Khatoon, Z., McTiernan, C. D., Suuronen, E. J., Mah, T.-F. & Alarcon, E. I. 2018. Bacterial biofilm formation on implantable devices and approaches to its treatment and prevention. *Heliyon* 4(12): e01067. https://doi.org/10.1016/j.heliyon.2018.e01067

Kusdianto, K., Puri, N. R., Shimada, M., Madhania, S. & Winardi, S. 2025. Synergistic effect of calcination temperature and silver doping on photocatalytic performance of ZnO material. *Materials* 18(14): 3362. https://doi.org/10.3390/ma18143362

Li, P., Yin, R., Cheng, J. & Lin, J. 2023. Bacterial biofilm formation on biomaterials and approaches to its treatment and prevention. *Preprints*. https://doi.org/10.20944/preprints202306.2248.v1

Talari, M. K., Majeed, A., Tripathi, D. K. & Tripathy, M. 2012. Synthesis, characterization and antimicrobial investigation of mechanochemically processed silver doped ZnO nanoparticles. *Chemical & Pharmaceutical Bulletin* 60(7): 818–824. https://doi.org/10.1248/cpb.c110479

Monegro, A. F., Muppidi, V. & Regunath, H. 2023. *Hospital Acquired Infections*. StatPearls Publishing. https://www.ncbi.nlm.nih.gov/books/NBK441857/

Puspasari, V., Ridhova, A., Hermawan, A., Amal, M. I. & Khan, M. M. 2022. ZnO-based antimicrobial coatings for biomedical applications. *Bioprocess and Biosystems Engineering* 45(9): 1421–1445. https://doi.org/10.1007/s00449-022-02733-9

Rashid, A. R. A., Shamsuri, N. A. F., Surani, A. H., Hakim, A. A. N. & Ismail, K. 2019. Zinc oxide coated polymer optical fiber for measuring uric acid concentrations. *Optoelectronics and Advanced Materials—Rapid Communications* 13(1–2): 63–68.

Rashid, A. R. A., Surani, A. H., Mukhtar, W. M., Arsad, N. & Menon, P. S. 2024. ZnO and GO coated plastic optical fiber for low concentration of ethanol detection in beer. *Optoelectronics and Advanced Materials—Rapid Communications* 18: 217–222.

Amrute, V., Monika, Supin, K. K., Vasundhara, M. & Chanda, A. 2024. Observation of excellent photocatalytic and antibacterial activity of Ag doped ZnO nanoparticles. *RSC Advances* 14(45): 32786–32801. https://doi.org/10.1039/d4ra05197a

Weber, M., Renkawitz, T., Voellner, F., Craiovan, B., Greimel, F., Worlicek, M., Grifka, J. & Benditz, A. 2018. Revision surgery in total joint replacement is cost-intensive. *BioMed Research International* 2018: 8987104. https://doi.org/10.1155/2018/8987104

Rashid, A. R. A., Hakim, A. A. N., Yahaya, N., & Surani, A. H. 2020. U-bent polymer optical fiber (POF) for Escherichia coli detection. Optoelectronics and Advanced Materials-Rapid Communications, 14(March-April 2020), 118-122.